ChemPubSoc Europe

DOI: 10.1002/chem.201703361

CHEMISTRY A European Journal Full Paper

Zeolites

Synthesis and Structure Determination of Large-Pore Zeolite SCM-14

Yi Luo,[a, b, c] Stef Smeets,[b] Fei Peng,[b] Ahmed S. Etman,[b] Zhendong Wang,*[a] Junliang Sun,*[b, d] and Weimin Yang*[a, c]

Abstract: SCM-14 (Sinopec Composite Material No. 14), a new stable germanosilicate zeolite with a 12×8×8-ring channel system, was synthesized using commercially available 4-pyrrolidinopyridine as organic structure-directing agents (OSDAs) in fluoride medium. The framework structure of SCM-14 was determined using rotation electron diffraction (RED), and refined against synchrotron X-ray powder diffraction (SXPD) data for both as-made and calcined materials. The framework structure of SCM-14 is closely related to that of three known zeolites: mordenite (**MOR**), GUS-1 (**GON**), and IM-16 (**UOS**). SCM-14 has the same projection as that of mordenite and GUS-1 when viewed along the 12-ring channels, and possesses two more straight 8-ring channels running perpendicular to the 12-ring channels. The structure of SCM-14 can be constructed by either the same layers as that of GUS-1 or the same columns as that of IM-16. Based on their structural relationship, three topologically reasonable hypothetical zeolites were predicted.

Introduction

Zeolites are a dominant class of crystalline microporous materials that are not only extensively applied in traditional fields such as catalysis, adsorption, and ion-exchange, but have also found applications in emerging areas like medicine, electricity, and luminescence.[1–3] The optimal performance of a zeolite in these applications is highly dependent on its physicochemical properties, such as its pore architecture, composition, and stability, which are essentially determined by its structure. Therefore, continuous effort has been devoted to the synthesis of new zeolites with diverse framework structures. Of particular interest is the size of the pores and dimensionality of the channel system. Zeolites are therefore often classified as small (8-membered rings, 8-ring), medium (10-ring), large (12-ring), or extra-large (12-ring or larger) pore materials.[4] Although considerable effort has been devoted to synthesize extra-large pore zeolites recently,[5–7] most of the industrial applications involving zeolites are focused on small (**LTA**, **CHA**), medium (**MFI**, **MWW**, **FER**), and large pore (**LTL**, **MOR**, **MTW**, **BEA**, **FAU**) materials. The large pore materials in particular dominate (>95%) of the synthetic zeolite market.[8,9] Therefore, in an attempt to expand the application of zeolites and provide alternative processes, synthesizing new large pore zeolite materials with diverse pore characters is still highly desirable.

In recent years, the major strategies to synthesize zeolites include 1) using a predesigned organic structure-directing agent (OSDA), and 2) introducing a fluoride mineralizer coupled with substituting framework silicon by germanium.[2] It is well known that OSDAs can act as templates when surrounded by inorganic species during the synthesis and thus play a crucial role in determining the formed zeolite structures. The size, shape, rigidity, and C/N ratio of the OSDA molecules greatly influence the pore size, pore dimension, and pore architecture of the synthesized zeolites.[10] On the other hand, compared with Si, Ge possesses more flexible T-O-T angles and longer T–O bonds, and favors the formation of small building units *d4r* (double 4-rings), which can significantly enrich the variety of structure topologies of zeolites.[11,12] Finally, the introduction of F^- further promotes the formation of *d4r* units and increases their stability.[13] The combination of these strategies has resulted in the formation of plenty of novel large and extra-large-pore germanosilicate zeolites.[14,15] However, the predesigned OSDAs employed in the synthesis are usually large, complex, expensive, and complicated to prepare. Once a potentially in-

[a] *Y. Luo, Dr. Z. Wang, Prof. W. Yang*
State Key Laboratory of Green Chemical Engineering and Industrial Catalysis
Sinopec Shanghai Research Institute of Petrochemical Technology
1658 Pudong Beilu, Shanghai 201208 (P. R. China)
E-mail: wangzd.sshy@sinopec.com
yangwm.sshy@sinopec.com

[b] *Y. Luo, Dr. S. Smeets, F. Peng, A. S. Etman, Prof. J. Sun*
Department of Materials and Environmental Chemistry
Stockholm University
106 91 Stockholm (Sweden)
E-mail: junliang.sun@pku.edu.cn

[c] *Y. Luo, Prof. W. Yang*
School of Chemical Engineering
East China University of Science and Technology
130 Meilong Road, Shanghai 200237 (P. R. China)

[d] *Prof. J. Sun*
College of Chemistry & Molecular Engineering
Peking University
No. 5 Yiheyuan Road, Beijing 100871 (P. R. China)

Supporting information and the ORCID identification number(s) for the author(s) of this article can be found under https://doi.org/10.1002/chem.201703361.

teresting new zeolite has been synthesized, researchers usually go through great efforts to replace these expensive OSDAs by simpler and cheaper ones to scale-up for commercial or industrial application.[16,17] Hence, synthesis of new large pore zeolites using simple and commercially available OSDAs at the beginning would be more favorable.

Herein, we report the synthesis of a new germanosilicate zeolite, named SCM-14, using a simple and commercially available organic amine as OSDA. SCM-14 is a large pore zeolite that contains a 3-dimensional 12×8×8-ring framework, built on the same layers as that of GUS-1 or the same columns as that of IM-16.[18–20] The layered features make the structures of SCM-14 and IM-16 ideal candidates for predicting zeolites with new topologies by inverse sigma transformation.[21]

Results and Discussion

SCM-14 was synthesized using commercially available 4-pyrrolidinopyridine as the OSDA in the presence of germanium and fluorine. During the initial experiments, GeO_2 always appeared in the product as an impurity. In order to avoid GeO_2, a two-step heating crystallization program (383 K for 1 day, and 443 K for 5 days) was applied. By using a gel composition of $1.0\,SiO_2$:$0.4\,GeO_2$:0.6 OSDA: 0.6 HF: $20\,H_2O$, a crystalline product with a low amount of amorphous material could be produced.

To demonstrate that the 4-pyrrolidinopyridine molecule is intact and incorporated in the zeolite structure, C, N, and H elemental analyses were performed on as-made SCM-14. It gave a C/N molar ratio value of 5.0, which is close to the expected C/N molar ratio for the OSDA molecule (C/N = 4.5), indicating that most of OSDA molecules remain intact (Table S1 in Supporting Information). This was corroborated by the ^{13}C solid-state MAS NMR spectra of as-made SCM-14 (Figure S1). Meanwhile, the ^{13}C liquid MAS NMR spectrum of OSDA molecules, pronated by acid in solution, and the initial molar ratio of OSDA/HF in the starting gel indicate that the OSDA molecules in SCM-14 were singly protonated by HF (SCM-14 crystallized in alkaline condition (pH 8.0≈9.0), Figure S1a–d). SCM-14 is stable after removing OSDAs by calcination in air (823 K). The argon adsorption analysis shows a major pore size of 0.56 nm (t-plot method, Figure S2), which is typical for zeolite structures with 12-ring pores.[22] The ^{29}Si solid-state MAS NMR spectra and ^{19}F solid-state NMR spectra, which are useful to obtain information about the local atomic environments, were also collected on as-made SCM-14. The ^{29}Si solid-state MAS NMR spectrum shows a peak centered at −107.8 ppm, demonstrating that all of the Si atoms in the framework are four-coordinated (Figure S3).[23] The ^{19}F NMR solid-state spectrum indicates the presence of *d4r* units in the framework structure of SCM-14, because of a strong peak centered at −7.2 ppm (Figure S4). Normally, this peak is attributed to the F^- located in the *d4r* units, and corresponds to an average presence of three or four Ge atoms in the *d4r* units (i.e., Si_5Ge_3- or Si_4Ge_4-*d4r*).[24] Another peak at −122.1 ppm can be assigned to fluorosilicate compound impurities in the outer surface of crystal or in the amorphous phase (Figure S4).[25] Meanwhile, it is worth noting that the area of these two peaks is almost the same ($S_{-7.2}/S_{-122}$ = 0.95), indicating significant F species in the impurities.

The structure determination of SCM-14 was carried out using the rotation electron diffraction (RED) method. A RED dataset was collected on a plate-like crystal (Figure 1), which is the typical morphology of SCM-14 (Figure S5). The RED data

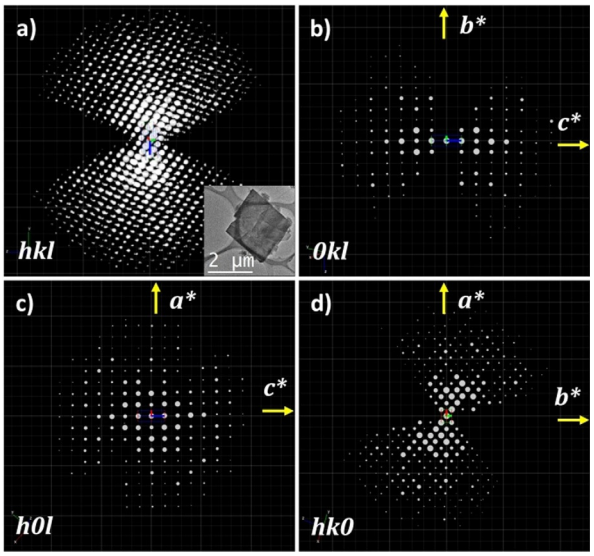

Figure 1. a) 3D reciprocal lattice of SCM-14 reconstructed from the RED data. The crystal from which the RED data was collected is shown in the insert. b–d) three 2D slices 0*kl*, *h*0*l*, and *hk*0 cut from the reconstructed reciprocal lattice. The reflection conditions can be deduced as *hkl*: $h+k=2n$, 0*kl*: $k=2n$, *h*0*l*: $h=2n$, *hk*0: $h+k$, and *h*00: $h=2n$. The possible space groups are *Cmmm*, *Cmm*2, and *C*222.

show that SCM-14 has a *C*-centered lattice with unit cell parameters of $a=17.51$, $b=21.28$, $c=7.61$ Å, $\alpha=89.95$, $\beta=90.62$, and $\gamma=89.98^\circ$ (Table S2). As presented in Figure 1, the reflection conditions were obtained from the 2-dimensional slices as 0*kl*, *h*0*l*, and *hk*0 with extinction symbol *C*−−−, and the possible space group could then be deduced to be *Cmmm*, *Cmm*2, or *C*222. When the RED data were cut at a resolution of 0.70 Å, the completeness remained as high as 79.5% in the *mmm* Laue class, which indicates a rather good quality of the RED data (Table S2). The structure of SCM-14 was initially solved in space group *Cmmm* using the zeolite-specific software Focus with the RED data.[26] Later, the same structural model was also produced by Sir2014,[27] which gave us confidence that the model was correct. All four symmetrically independent framework T atoms (Si, Ge) and ten bridging O atoms were located, and the coordinates of the atoms were optimized geometrically using the program DLS-76.[28]

The synchrotron X-ray powder diffraction (SXPD) data of as-made and calcined zeolite SCM-14 were both collected for Rietveld refinement,[29] to confirm the structure model and obtain more structural information about the OSDAs. Before the refinement, the SXPD data of both as-made and calcined SCM-14 were indexed using the LSI-index method implemented in the software Topas.[30] An orthorhombic *C*-centered unit cell was obtained (as-made: extinction symbol *C*—, $a=17.087$,

$b = 21.156$, $c = 7.534$ Å; calcined: extinction symbol C—, $a = 17.169$, $b = 21.047$, $c = 7.564$ Å), which is consistent with the unit cell obtained from the RED data.

Rietveld refinement was initiated using the geometrically optimized framework coordinates in the software Topas.[31] The structure model with space group *Cmmm* exhibits T-O-T angles of 180° because some O atoms lie on an inversion center. By reducing the symmetry to the subgroups *Cmm*2 or *C*222, the 180° bond angle constraint could be released, leading to more favorable T-O-T angles and a better profile fit. After trial and error, it was found that space group *C*222 fits best with the SXPD data, and was therefore selected for the structure refinement of zeolite SCM-14. Soft geometric restraints were applied on all the bond distances and angles of the framework atoms. These restraints were imposed throughout the refinement, but their relative weighting with respect to the SXPD data was reduced as the refinement progressed.

For calcined SCM-14, the final refinement converged with agreement values $R_B = 0.014$, $R_{wp} = 0.123$, and $R_{exp} = 0.118$ (Figure 2, Table 1) and the subtle differences between the observed and calculated patterns can be assigned to problems

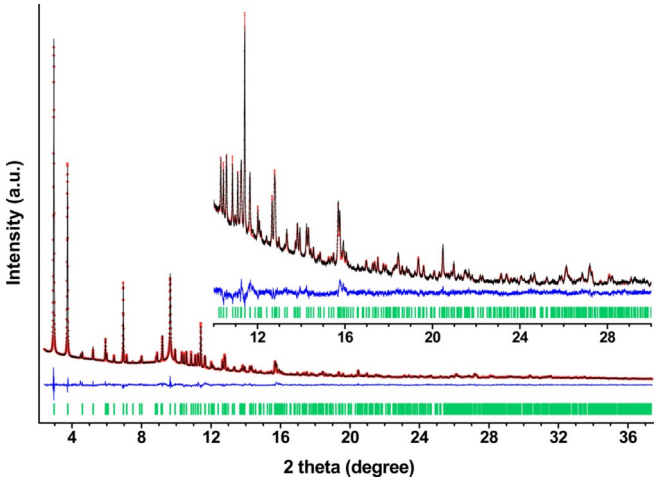

Figure 2. Observed (red points), calculated (black line), and difference (blue line) profiles for the Rietveld refinement of calcined SCM-14. The profiles in the inset have been scaled up by a factor of 5 to show more detail.

with the description of the peak shape. All of the bond distances and angles in the refined structure of calcined SCM-14 are chemically reasonable (Table S3). The refined chemical composition of calcined SCM-14 is $[Si_{36.0}Ge_{12.0}O_{96.0}]$ (Si/Ge = 3.0). It was found that the Ge atoms were almost exclusively located on the *d4r* units (94.6%), with an average composition of $Si_{5.1}Ge_{2.9}$, which matches well with the ^{19}F NMR spectroscopy result ($Si_{5.0}Ge_{3.0}$). However, the Si/Ge molar ratio of the framework obtained from the refinement is slightly lower than that of the ICP result (Table S1), perhaps because of some unreacted or amorphous material.

The guest species F^-, OSDAs, and any potential H_2O in the framework structure were located by means of the Rietveld refinement of as-made SCM-14. The chemical composition of the as-made SCM-14 sample can be roughly calculated as

Table 1. Crystallographic and experimental parameters for calcined and as-made SCM-14 (SXPD).

Parameters	Calcined	As-made
composition	$[Si_{36.0}Ge_{12.0}O_{96}]$	$\lvert(C_9N_2H_{13}F)_2(H_2O)_{1.0}\rvert[Si_{36.0}Ge_{12.0}O_{96}]$
space group	*C*222	*C*222
a [Å]	17.1814(2)	17.0776(3)
b [Å]	21.0734(3)	21.1489(4)
c [Å]	7.5720(9)	7.5350(2)
V [Å^3]	2741.72(7)	2721.46(9)
2θ range [°]	2.4 to 37.4	2.4 to 37.4
wavelength [Å]	0.68950	0.68950
R_B	0.014	0.020
R_{wp}	0.123	0.164
R_{exp}	0.118	0.132
GoF	1.043	1.243
observations	9012	9012
contributing reflections	688	688
parameters	106	147
restraints	74	95

$\lvert(C_9N_2H_{13}F)_{1.99}(H_2O)_{0.84}\rvert[Si_{37.8}Ge_{10.2}O_{96}]$ (Table S1, Figure S6). The contents of Ge, OSDA, and H_2O were calculated based on the ICP, CHN elemental analysis, and TGA, respectively. The occupancy of F^- in the four *d4r* units was fixed at 0.5, to maintain charge-balance with the OSDA, and their locations were fixed at the center of *d4r* unit. To find the location of OSDA, an idealized model of OSDA was generated using ChemBio 3D,[32] and then added to the SCM-14 structure model as a rigid body. The approximate location and occupancy of OSDA and H_2O in the channel were found using the simulated-annealing algorithm in software Topas, following the procedure described by Smeets et al.[33] The final refinement converged with agreement values $R_B = 0.020$, $R_{wp} = 0.164$, and $R_{exp} = 0.132$ (Table 1, Figure S7). All of the bond distances and angles in the refined structure of as-made SCM-14 are chemically reasonable (Table S4). The chemical composition of as-made SCM-14 refined to $\lvert(C_9N_2H_{13}F)_{2.0}(H_2O)_{1.0}\rvert[Si_{36.0}Ge_{12.0}O_{96}]$.

The obtained OSDAs were disordered under the symmetry of *C*222, but fit well into the channels of SCM-14 (Figure 3). There are several reasons that may lead to the disordered guest molecules: 1) the determined cell is a sub-cell of the real structure; 2) the arrangement of OSDAs is ordered but their symmetry is lower than that of the framework structure; 3) the OSDAs are distributed randomly and without long range order in the channels. However, close inspection of the single crystal RED and SXPD data revealed no evidence for a supercell. Meanwhile, we found that the refined disordered arrangement of OSDAs actually consists of four different types of ordered arrangements, and each type of them has an occupancy of 25% (Figure 3a). This means that the arrangement of OSDAs is unlikely to be completely disordered in the channels, and the lower symmetry of the OSDAs could be the real reason, which is a quite common phenomenon for zeolitic materials.[33–35]

SCM-14 zeolite possesses a three-dimensional channel system with straight 12-ring and 8-ring channels along the *c*-axis which are intersected by 8-ring channels running along the *a*- and *b*-axes (Figure 4), giving it a framework density of

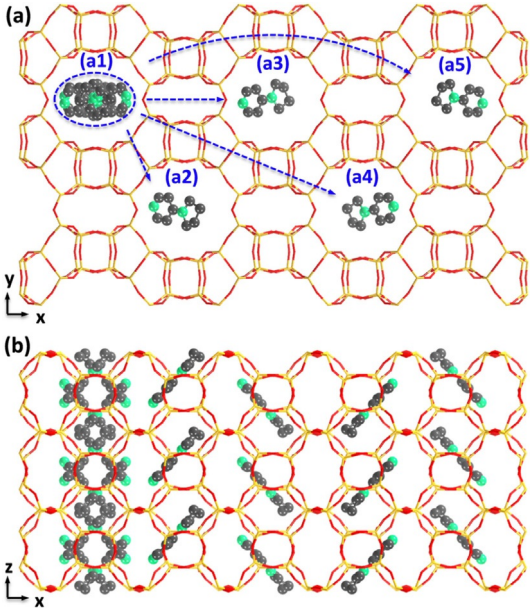

Figure 3. Location of OSDAs in the channels of SCM-14. Their arrangement is disordered under symmetry *C*222 (a1, blue ellipse), but can be viewed as four different types of ordered arrangements (a2–5), and each type has an occupancy of 25%. (b) Arrangement of the OSDAs viewing along the *b*-axis.

17.5 T atoms per 1000 Å^3. The effective pore diameters of the 12-ring and 8-ring channels along the *c*-axis are 7.2×6.3 and 5.2×1.5 Å, respectively, while the 8-ring channels along the *a*- and *b*-axes have openings of 4.9×2.6 and 4.9×1.7 Å, respectively, considering an oxygen radius of 1.35 Å. It could be seen that the projection of 12-ring and 8-ring channels along the *c*-axis in the framework structure of SCM-14 is the same as those of zeolites GUS-1 and mordenite (Figure S8a–c), and that they all possess quite similar pore sizes. After closer comparison, we found that the layers containing the 12-ring channels in SCM-14 are also present in GUS-1, and that SCM-14 can be formed

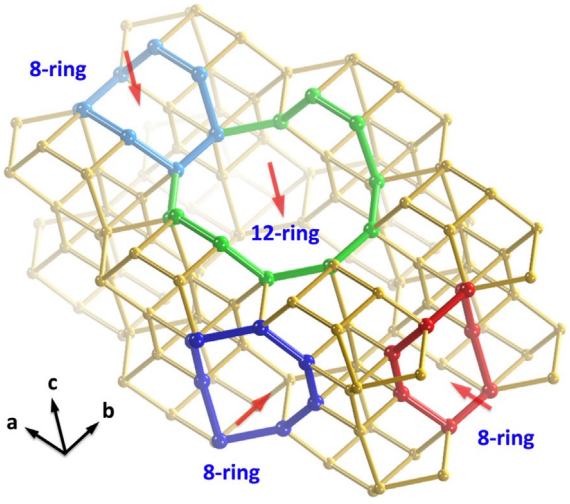

Figure 4. The framework structure of SCM-14. The pores with different ring sizes are highlighted in different colors. The channel directions are pointed out by the red arrows (O atoms have been omitted for clarity).

from GUS-1 through a sigma expansion.[36] In this way, two more straight 8-ring channels along *a*- and *b*-directions are formed, resulting in the 3D channel system found in SCM-14.

The relation between the structures of SCM-14 and GUS-1 is depicted in Figure 5, and can be easily seen by comparing the

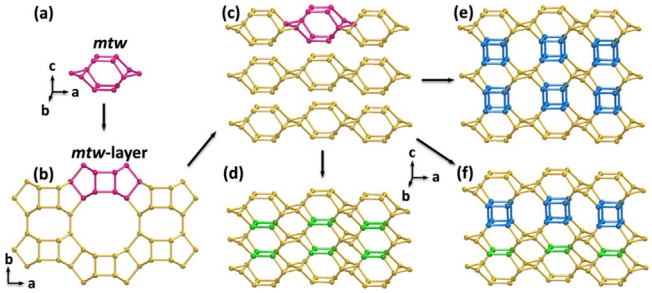

Figure 5. Structures of SCM-14, GUS-1, and SCM-14-P1. (a) Composite building unit *mtw*. (b) View of the *mtw*-layer and structures along the *c*-axis. (c) Tilt view of the stacked *mtw*-layer. (d) GUS-1: condensation of the layers through the single 4-ring, forming the 6-ring. (e) SCM-14: Connection of the layers by bridging O atoms on the single 4-ring, forming *d4r* and the 8-ring. (f) SCM-14-P1: Alternative connection of the layers by single 4-ring and *d4r*, forming 6-ring and 8-ring. The bonds with different colors highlight the possible connections different frameworks (O atoms have been omitted for clarity).

[0 1 0] and [0 0 1] projections. They share the same *mtw*-layer that can be constructed by *mtw* units (Figure 5a–c). In the case of GUS-1, each layer is connected to the two neighboring ones through a shared single 4-ring to form straight 6-ring pores running parallel to the *b*-axis (Figure 5d, green). For SCM-14 however, the layers are connected through bridging O atoms between the unsaturated 4-ring, giving rise to *d4r* units (Figure 5e, blue). As a consequence, the 6-ring pores in GUS-1 are expanded to 8-ring pores in SCM-14. Furthermore, based on the stacking relationship that has been demonstrated between ITQ-33, ITQ-44, and NUD-1,[7] a new structure SCM-14-P1 can be predicted. In SCM-14-P1, the connection of neighboring layers through alternatively sharing single 4-ring and *d4r* units results in a new hypothetical zeolite possessing structural features of both SCM-14 and GUS-1 (Figure 5f). Meanwhile, by stacking in this manner, a new column constructed from *mtw* and *d4r* units can be formed, equivalent to the one that exists in the structure of ITQ-7 (**ISV**) (Figure S9).[37] This makes the structure of predicted zeolite SCM-14-P1 rather reasonable from the topological point of view.

On the other hand, the structure of SCM-14 is also closely related to that of IM-16 as they share the same *mtw-d4r*-column with alternating *mtw* and *d4r* units (Figure 6a). The main difference between these two structures lies in the arrangement of *mtw-d4r*-columns. In SCM-14, the connection of the neighboring *mtw-d4r*-columns is established through a crankshaft-wise arrangement to form SCM-14-layers (Figure 6b). Then the SCM-14-layers are condensed together through bridging O atoms on the mirror plane, resulting in 12- and 8-ring pores along the *c*-axis (Figure 6d). In the structure of IM-16, the connection of *mtw-d4r*-columns obeys a stepwise arrangement to form the IM-16-layers (Figure 6c). The IM-16-layers are also

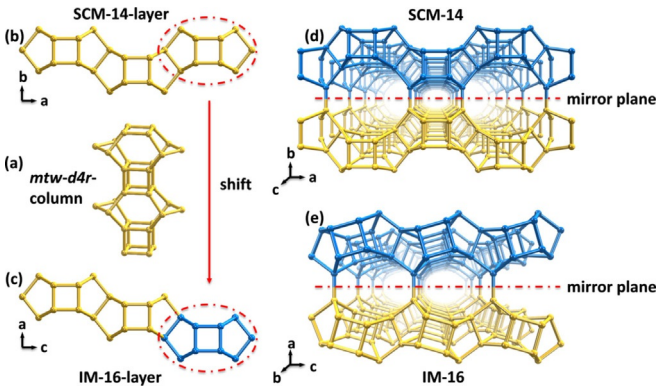

Figure 6. Relationship between SCM-14 and IM-16. (a) A column formed by *mtw* and *d4r*. (b) SCM-14-layer: *mtw-d4r*-columns constructed via a crankshaft-wise arrangement. (c) IM-16-layer: *mtw-d4r*-columns constructed through a stepwise arrangement. (d) Perspective view of SCM-14: connection of the SCM-14-layers by bridging O atoms on the mirror plane. (e) Perspective view of IM-16: connection of the IM-16-layers by bridging O atoms on the mirror plane. The ellipses and different colors were used to highlight the relationship between the zeolites (O atoms have been omitted for clarity).

connected together through bridging O atoms on the mirror plane, giving rise to 10-ring pores along the *b*-axis (Figure 6e). When viewed along the *a*-axis, it is worth noting that the structure of IM-16 also possesses a *mtw*-layer that is distinctly different from the one found in SCM-14 (Figure S10a–c). These layers are connected by bridging O atoms between the unsaturated single 4-ring give rise to *d4r* units (Figure S10e) and 8-ring pores. Inspired by the relationship between GUS-1, SCM-14, and SCM-14-P1 as discussed above, two new zeolite structures SCM-14-P2 and SCM-14-P3 were predicted through inverse sigma expansion (Figure S10d and f). The structural relationships between IM-16, SCM-14-P2, and SCM-14-P3 are the same as those shown in Figure 5.

Conclusion

A new stable germanosilicate zeolite SCM-14 with an interesting topology has been synthesized using 4-pyrrolidinopyridine as OSDA. Its structure was determined using RED data, and confirmed through Rietveld refinement using SXPD data, from which the OSDAs were also located.

Zeolite SCM-14 possesses a 3D framework structure with a 12×8×8-ring channel system. Its framework structure has the same projection along the *c*-axis as that of mordenite and GUS-1, but possesses two straight 8-ring channels running perpendicular to the *c*-axis. This may give SCM-14 promising shape selective and diffusion properties for particular applications. Based on the structural relationship between the framework of SCM-14 and those of GUS-1 and IM-16, three new zeolite frameworks were hypothesized. Further exploration of the potential application of SCM-14 and the synthesis of the predicted zeolites is in progress.

Experimental Section

Zeolite synthesis

In the typical synthesis of zeolite SCM-14, Ludox (SiO_2, HS-40, 40% Sigma–Aldrich), 4-pyrrolidinopyridine (OSDA, 98.0%, Shanghai Di Bo chemical technology Co., Ltd), GeO_2 (99.0%, Sinopharm Chemical Reagent Co., Ltd), HF (40% in water solution, Sinopharm Chemical Reagent Co., Ltd), and distilled water were used as source materials. Firstly, GeO_2 and 4-pyrrolidinopyridine were added to distilled water, and the mixture was stirred at room temperature until all the GeO_2 and 4-pyrrolidinopyridine were dissolved. Secondly, Ludox was added dropwise while stirring. After the gel became homogeneous, HF was introduced and the resulting gel has a composition of 1 SiO_2:0.4 GeO_2:0.6 OSDA:0.6 HF:20 H_2O. Finally, the mixture was aged at 353 K for 2 hours, and then transferred into a 23 mL Teflon-lined stainless-steel autoclave. The autoclave was sealed and the mixture allowed to crystallize at 383 K for 1 day and subsequently at 443 K for 5 days under dynamic condition (rotation oven, 20 rpm). After the crystallization finished, the autoclave was quenched with cold water and the solid product was recovered by centrifugation, washed with deionized water, and then dried at 383 K for 12 hours. The recovered solid product was then analysed for purity and crystallinity using powder X-ray diffraction. The organic molecules and fluoride occluded in the framework were removed by calcination at 832 K for 5 h in air atmosphere.

Characterization

Synchrotron X-ray powder diffraction (SXPD) data of as-made and calcined SCM-14 zeolites were collected in a 0.5 mm capillary on the BL14B1 X-ray diffraction beamline at the Shanghai Synchrotron Radiation Facility in Shanghai, China using a wavelength of 0.68950 Å. The SXPD patterns were collected in the 2θ range 2.4–37.4° with 0.004° data binning. Single-crystal rotation electron diffraction (RED) data were collected on a 2.5×2.5×0.2 μm crystal of as-made SCM-14 using the RED software on a JEOL JEM2100 TEM operated at 200 kV.[38,39] The goniometer tilt range is from −68.8° to 65.8° (exposure time 0.5 s), and in total 737 ED patterns were recorded with a step of 0.2°. The reciprocal space reconstruction and reflection intensity extraction were carried out using the RED software.[40]

Scanning electron microscopy (SEM) images were taken on a field emission XL30E scanning electron microscopy (FEI Company). Liquid ^{13}C NMR spectra were recorded on a Bruker AV-400 spectrometer. ^{29}Si solid-state MAS NMR spectra were acquired on a Varian Model VNMRS-400WB spectrometer with a 7.5 mm probe at 79.43 MHz and a spinning rate of 3 kHz. ^{13}C solid-state MAS NMR spectra were recorded a Varian Model VNMRS-400WB spectrometer with a 7.5 mm probe at 100.54 MHz and a spinning rate of 5 kHz. ^{19}F solid-state NMR spectra were recorded on a Bruker AVANCEIII 500WB spectrometer with a 2.5 mm probe at 376.5 MHz with a spinning rate of 30 kHz. The amounts of Si and Ge were quantified by inductively coupled plasma (ICP) on a Varian 725-ES instrument after dissolving the samples in HF solution. Elemental analyses of C, N, and H were conducted on an ElementarVario MICRO CUBE elemental analyzer. Argon adsorption experiments were performed on a MICROMERITICS ASAP2010 Accelerated Surface Area & Porosimetry System. The DSC-TGA curves were obtained by a SDT Q600 V20.9 Build 20 thermal analyzer. Samples were exposed to air atmosphere where temperature was elevated from 303 to 1173 K at a rate of 10 K min^{-1}.

Acknowledgements

The authors gratefully acknowledge Jianqiang Wang and the beamline scientists (beamline BL14B1 at the SSRF, Shanghai, China, and beamline I11 at Diamond, Didcot, UK), for their assistance with the SXPD experiment. The authors acknowledge financial support from the China Petrochemical Corporation (Sinopec Group), the National Natural Science Foundation of China (project numbers: 21503280, 21527803, 21471009, 21321001), the China Scholarship Council (CSC), and the Swiss National Science Foundation (project number: 165282).

Conflict of interest

The authors declare no conflict of interest.

Keywords: organic structure-directing agent · Rietveld refinement · structure determination · synthesis · zeolites

[1] M. E. Davis, *Nature* **2002**, *417*, 813 – 821.
[2] J. Li, A. Corma, J. Yu, *Chem. Soc. Rev.* **2015**, *44*, 7112 – 7127.
[3] M. E. Davis, *Chem. Mater.* **2014**, *26*, 239 – 245.
[4] C. C. Freyhardt, R. F. Lobo, S. Khodabandeh, J. E. Lewis, M. Tsapatsis, M. Yoshikawa, M. A. Camblor, M. Pan, M. M. Helmkamp, S. I. Zones, M. E. Davis, *J. Am. Chem. Soc.* **1996**, *118*, 7299 – 7310.
[5] J. Jiang, Y. Xu, P. Cheng, Q. Sun, J. Yu, A. Corma, R. Xu, *Chem. Mater.* **2011**, *23*, 4709 – 4715.
[6] J. Jiang, Y. Yun, X. Zou, J. L. Jorda, A. Corma, *Chem. Sci.* **2015**, *6*, 480 – 485.
[7] F.-J. Chen, Y. Xu, H.-B. Du, *Angew. Chem. Int. Ed.* **2014**, *53*, 9592 – 9596; *Angew. Chem.* **2014**, *126*, 9746 – 9750.
[8] S. I. Zones, *Microporous Mesoporous Mater.* **2011**, *144*, 1 – 8.
[9] W. Vermeiren, J.-P. Gilson, *Top. Catal.* **2009**, *52*, 1131 – 1161.
[10] M. Moliner, F. Rey, A. Corma, *Angew. Chem. Int. Ed.* **2013**, *52*, 13880 – 13889; *Angew. Chem.* **2013**, *125*, 14124 – 14134.
[11] M. O'Keeffe, O. M. Yaghi, *Chem. Eur. J.* **1999**, *5*, 2796 – 2801.
[12] G. O. Bnmner, W. M. Meier, *Nature* **1989**, *337*, 146 – 147.
[13] R. M. Shayib, N. C. George, R. Seshadri, A. W. Burton, S. I. Zones, B. F. Chmelka, *J. Am. Chem. Soc.* **2011**, *133*, 18728 – 18741.
[14] J. Jiang, J. Yu, A. Corma, *Angew. Chem. Int. Ed.* **2010**, *49*, 4986 – 4988; *Angew. Chem.* **2010**, *122*, 5106 – 5108.
[15] W. Hua, H. Chen, Z.-B. Yu, X. Zou, J. Lin, J. Sun, *Angew. Chem. Int. Ed.* **2014**, *53*, 5868 – 5871; *Angew. Chem.* **2014**, *126*, 5978 – 5981.
[16] R. Bai, Q. Sun, N. Wang, Y. Zou, G. Guo, S. Iborra, A. Corma, J. Yu, *Chem. Mater.* **2016**, *28*, 6455 – 6458.
[17] X. Meng, F.-S. Xiao, *Chem. Rev.* **2014**, *114*, 1521 – 1543.
[18] J. Plévert, Y. Kubota, T. Honda, T. Okubo, Y. Sugi, *Chem. Commun.* **2000**, *0*, 2363 – 2364.
[19] Y. Lorgouilloux, M. Dodin, J.-L. Paillaud, P. Caullet, L. Michelin, L. Josien, O. Ersen, N. Bats, *J. Solid State Chem.* **2009**, *182*, 622 – 629.
[20] F. Raatz, E. Freund, C. Marcilly, *J. Chem. Soc. Faraday Trans. 1* **1983**, *79*, 2299 – 2309.
[21] D. P. Shoemaker, H. E. Robson, L. Broussard, *Proceedings of the Third International Conference on Molecular Sieves*, (Eds.: J. B. Uytterhoeven), Leuven University Press, **1973**, pp. 138 – 143.
[22] C.-Y. Chen, L. W. Finger, R. C. Medrud, C. L. Kibby, P. A. Crozier, I. Y. Chan, T. V. Harris, L. W. Beck, S. I. Zones, *Chem. Eur. J.* **1998**, *4*, 1312 – 1323.
[23] T. Blasco, A. Corma, M. J. Díaz-Cabañas, F. Rey, J. A. Vidal-Moya, C. M. Zicovich-Wilson, *J. Phys. Chem. B* **2002**, *106*, 2634 – 2642.
[24] A. Pulido, G. Sastre, A. Corma, *ChemPhysChem* **2006**, *7*, 1092 – 1099.
[25] D. L. Dorset, G. J. Kennedy, K. G. Strohmaier, M. J. Diaz-Cabañas, F. Rey, A. Corma, *J. Am. Chem. Soc.* **2006**, *128*, 8862 – 8867.
[26] S. Smeets, L. B. McCusker, C. Baerlocher, E. Mugnaioli, U. Kolb, *J. Appl. Crystallogr.* **2013**, *46*, 1017 – 1023.
[27] M. C. Burla, R. Caliandro, B. Carrozzini, G. L. Cascarano, C. Cuocci, C. Giacovazzo, M. Mallamo, A. Mazzone, G. Polidori, *J. Appl. Crystallogr.* **2015**, *48*, 306 – 309.
[28] C. Baerlocher, A. Hepp, W. M. Meier, *DLS-76* **1976**.
[29] L. B. McCusker, R. B. Von Dreele, D. E. Cox, D. Louër, P. Scardi, *J. Appl. Crystallogr.* **1999**, *32*, 36 – 50.
[30] A. A. Coelho, *J. Appl. Crystallogr.* **2003**, *36*, 86 – 95.
[31] A. A. Coelho, *Topas-Academic v5.0* **2012**, http://www.topas-academic.net/.
[32] S. M. Kerwin, *J. Am. Chem. Soc.* **2010**, *132*, 2466 – 2467.
[33] S. Smeets, L. B. McCusker, C. Baerlocher, S. Elomari, D. Xie, S. I. Zones, *J. Am. Chem. Soc.* **2016**, *138*, 7099 – 7106.
[34] A. Burton, R. J. Darton, M. E. Davis, S.-J. Hwang, R. E. Morris, I. Ogino, S. I. Zones, *J. Phys. Chem. B* **2006**, *110*, 5273 – 5278.
[35] S. Smeets, L. B. McCusker, *Location of Organic Structure-Directing Agents in Zeolites Using Diffraction Techniques in Structure and Bonding*, Springer Berlin Heidelberg, Berlin, Heidelberg, **2017**, pp. 1 – 31.
[36] G. S. Lee, Y. Nakagawa, S. J. Hwang, M. E. Davis, P. Wangner, L. Beck, S. I. Zones, *J. Am. Chem. Soc.* **2002**, *124*, 7024 – 7034.
[37] L. A. Villaescusa, P. A. Barrett, M. A. Camblor, *Angew. Chem. Int. Ed.* **1999**, *38*, 1997 – 2000; *Angew. Chem.* **1999**, *111*, 2164 – 2167.
[38] D. Zhang, P. Oleynikov, S. Hovmöller, X. Zou, *Z. Krist. Int. J. Struct. Phys. Chem. Asp. Cryst. Mater.* **2010**, *225*, 94 – 102.
[39] W. Wan, J. Sun, J. Su, S. Hovmöller, X. Zou, *J. Appl. Crystallogr.* **2013**, *46*, 1863 – 1873.
[40] W. Wan, J. Sun, S. Hovmöller, X. Zou. *The Rotation Electron Diffraction (RED) Software Package*, **2012**. http:///www.calidris-em.com.

Manuscript received: July 20, 2017
Accepted manuscript online: October 2, 2017
Version of record online: November 3, 2017